*Progress In Electromagnetics Research C, Vol. 116, 81–93, 2021*

# Complementary Split Ring Resonator Based Massive MIMO Antenna System for 5G Wireless Applications

**Surendra Loya[1, 2, *] and Habibulla Khan[3]**

**Abstract**—A MIMO antenna for smartphones with radiation diversity is presented in this article. The proposed design consists of dual-fed Complementary Split Ring Resonator metamaterial antenna components in design, which is located at the edges of an FR-4 substrate. The total dimension is 75 mm × 150 mm × 1.6 mm. 50-ohm dual microstrip feed lines placed orthogonal to each other are used to feed the SRR. Due to this orthogonality, radiation diversity is easily achieved. The proposed structure is operated in dual bands from 3.43 GHz to 3.62 GHz and 4.78 GHz to 5.04 GHz. In both bands, good impedance bandwidth with a reasonable gain is achieved. The entire structure is simulated using CST EM software. All the simulated results are presented, which clearly show that the proposed structure is a good candidate for the future smartphone massive MIMO application.

## 1. INTRODUCTION

Multiple Input Multiple Output (MIMO) technology has played a vital role in recent past two decades. The reason for such an exponential development of MIMO antenna in the present-day communication world is that it can provide huge data rates and maintain the available spectrum more efficiently without demanding the bandwidth and transmission power [1, 2]. As mentioned above, the MIMO technology becomes a hopeful technology for communications devices which are going to be operated in the 5G spectrum [3, 4]. The 4G device, which uses LTE (Long-Term Evolution) for its operation, uses MIMO technology. The antenna used in 4G portable devices [5, 6] operates in multiple bands. Two to four elements are used in the MIMO, whereas in massive MIMO, a larger number of antennae are used. The massive MIMO is more spectral and energy efficient compared to the MIMO, and therefore, it occupies the entire 5G communication technology.

The commercial mobile headset that uses the fourth generation wireless communication is based on a $2 \times 2$ MIMO antenna system [7]. But the $2 \times 2$ MIMO is not a potential candidate for the 5G standard due to its high data rave and link reliability [8]. The 5G handset with $2 \times 2$ or $4 \times 4$ MIMO antenna systems can be operated to 4G standard. For 5G operation, the handset is really in need of more than 4 MIMO antennae [9], which is considered as massive MIMO. For providing good reliability, multiplexing gain, and diversity, the 5G handset requires at least 6 multiple antenna systems [10]. The reliable communication can be easily achieved with the help of better channel capacity, special diversity with multiplexing capability, and therefore with the massive MIMO technology the multipath fading [11, 12] is reduced. The throughput is also increased as the result of reduced multipath fading.

The C band from 3.4 GHz to 3.6 GHz is allotted as the frequency band for the future 5G communication [13]. Since the allocated band is less than 6 GHz, it is otherwise called a sub-6 GHz band. In many countries, the LTE band 42 and 43 are also under consideration for realizing the 5G massive MIMO. The LTE 42 band of operation ranges from 3.4 GHz to 3.6 GHz, and LTE 43 band

*Received 28 July 2021, Accepted 1 October 2021, Scheduled 10 October 2021*
* Corresponding author: Surendra Loya (surendra.loya2007@gmail.com).
[1] E.C.E., Usha Rama College of Engineering and Technology, India. [2] K.L. (Deemed to be University), Guntur, India. [3] E.C.E., Koneru Lakshmaiah Education Foundation, Guntur, India.

of operation is from 3.6 GHz to 3.8 GHz. For realizing the 5G massive MIMO, the ETU (European Telecommunication Union) chooses the frequency from 3.4 GHz to 3.8 GHz; China selects the frequency from 3.4 GHz to 3.6 GHz; and Korea selects the frequency from 3.4 GHz to 3.7 GHz [14, 15]. Several mobile terminal antennas designed for sub-6 GHz massive MIMO have been reported [12–14]. An 8-element antenna array for LTE band 42 has been studied in [12], and its measured ergodic channel capacity (for a $2 \times 8$ MIMO channel) has reached approximately 16 bps/Hz with a 20-dB signal-to-noise ratio (SNR). However, the antenna elements are placed along all four edges of a handset, and no other available spaces are reserved for the 4G antennas.

In the literature from [16–18], several massive MIMO antennas are proposed for the sub-6 GHz standard. In [16], an antenna array having 8 antennas is designed to operate at LTE 42, and all the antenna are placed with the edges. In [17], a 10 element array is proposed to operate at both 42 and 43 LTE bands. In [18], a MIMO array with 8 ports is designed to operate at 2.6 GHz with polarization orthogonality. In [19–23], massive MIMO antennas are proposed for 5G mobile handset. In [32], the proposed Ultra-Wide Band (UWB) MIMO antenna with two stubs in the ground plane is used to improve the impedance matching, and a Complementary Split Ring Resonator (CSRR) is etched in the ground plane for improving the isolation at the resonating band. In [33], a cardia pacing circuit based on an implantable antenna is proposed in which CSRR is used for miniaturization. In [34], a simple 8 element UWB MIMO antenna with band rejection of 3G, 4G, and 5G bands using a stub is presented, and in [35], an 8 element UWB antenna with a simple patch structure is proposed, and a CSRR is etched in the ground for size miniaturization. In all the above references, the impedance bandwidth is not wide to cover both the LTE and 5G bands; the interelement isolation of the designed antenna is very low; and space is not fully exploited. So, there is a large scope for antenna engineers to design an antenna which covers the LTE and 5G bands along with good antenna efficiency and interelement isolation.

In this article, a dual-band massive MIMO-8 port antenna array is designed. The proposed antenna structure is capable of operating in two different bands that cover both the sub-6 GHz and LTE bands, which is the major requirement for the future 5G mobile handsets. The antenna is integrated into the handset Printed Circuit Board (PCB), and it also uses the CSRR metamaterial [24–31, 36, 37]. The entire structure is designed in CST EM studio. The modification in ground has a direct effect on inter element isolation and impedance matching. Since in most of the handsets the ground is fixed, it is not considered in the analysis.

## 2. PROPOSED ANTENNA DESIGN

The proposed antenna has four evolution stages, namely antennas A, B, C, and D. The proposed antenna is designed on an FR4 substrate with 4.4 as its $\varepsilon_r$ value. Antenna A is the seed antenna of the proposed 8 port massive MIMO antenna. Antenna A is a simple circular slot antenna. The length and width of antenna A is 34 mm. The thickness of the FR4 substrate used to design antenna A is 1.6 mm. The antenna is fed with dual microstrip feed, which are designed orthogonal to each other. Antenna A is depicted in Figure 1 along with its parameters. The proposed antenna is designed for 3.6 GHz. The parameter values are $W = L = 34$ mm, $W_F = 3$ mm, $L_F = 11.5$ mm, $R_1 = 9.25$ mm, $R_2 = 8$ mm,

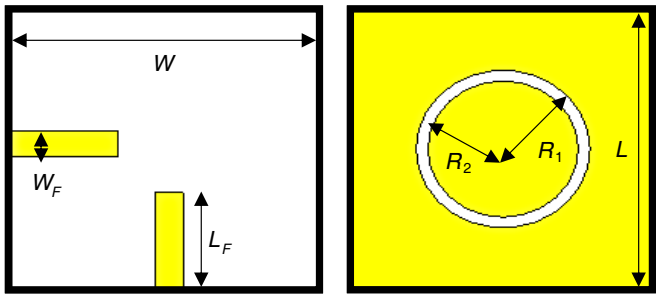


**Figure 1.** Antenna A.

$R_3 = 7.25\,\text{mm}$, $R_4 = 6\,\text{mm}$, $S = 0.25\,\text{mm}$, $ws = 1.25\,\text{mm}$, $W_{\text{mimo}} = 150\,\text{mm}$, $L_{\text{mimo}} = 75\,\text{mm}$.

$W$ and $L$ are the width and length of the ground and substate (antenna A); $W_F$ and $L_F$ are the width and length of the feed (antenna A); $R_1$ and $R_2$ are the outer and inner radii of the first ring (antenna A); $R_3$ and $R_4$ are the outer and inner radii of the second ring (antenna B); $S$ is the slit width of the CSRR; $ws$ is the width of the CSRR ring; $W_{\text{mimo}}$ and $L_{\text{mimo}}$ are the width and length of the final proposed MIMO antenna. The antenna configuration contains a pair of microstrip feed lines and a CSRR radiator in the ground plane. The length of the feed line was calculated using $L_F = \lambda_g/4 = c/4f_0\sqrt{\varepsilon_r}$, where $f_0 \approx 3.5\,\text{GHz}$, and $\varepsilon_r$ is the relative permittivity of the substrate. $W_F$ is the width of the feed which is calculated using the standard microstrip design equations. The calculation of effective radius and resonant frequency of the slot is governed by $Fr = (1.8412 * C)/2\Pi ae\sqrt{\varepsilon_r}$, where $ae$ is the effective radius of the slot derived from the circular patch equation, and $\varepsilon_r$ is the relative permittivity of the substrate. Figure 2 illustrates the antenna $S$-parameters. From the above observations, it is clear that for $S_{11} \leq -10\,\text{dB}$, the antenna provides impedance bandwidth 3.4–3.8 GHz. In addition, the mutual coupling characteristic of the dual-port design is less than $-15\,\text{dB}$ at the antenna resonance frequency (3.6 GHz).

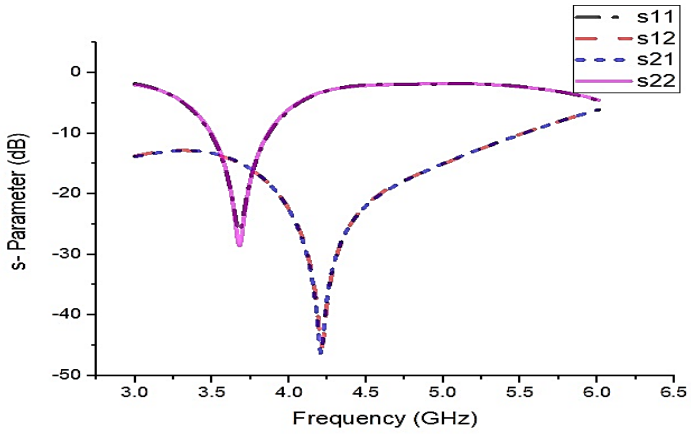


**Figure 2.** Simulated $S$-parameter of Antenna A (all $S_{11}$, $S_{12}$, $S_{21}$, and $S_{22}$).

Antenna B is a dual circular ring slot antenna. Another slot of radius 7.25 mm with thickness of 1.25 mm is etched. The dual ring circular slot antenna is fed with the microstrip feed placed orthogonal to each other. The feed line dimension used in antenna B is the same as antenna A. The proposed structure has very good impedance matching compared to antenna A. There is a shift in the operating frequency due to additional slot, which increases the capacitance of the proposed antenna structure. The isolation of antenna B is also very much improved in the entire operating band compared with antenna A. Antenna B is depicted in Figure 3, and the return loss performance of antenna B is presented in Figure 4.

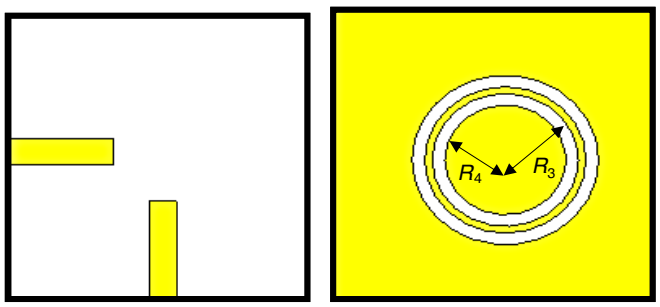


**Figure 3.** Antenna B.

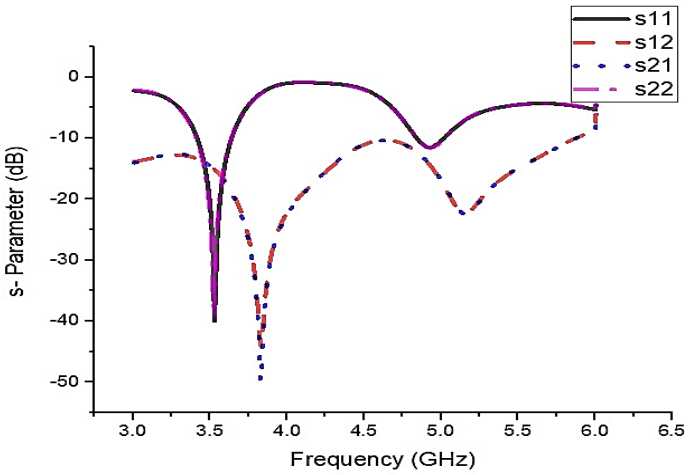


**Figure 4.** Simulated $S$-parameter of Antenna B (all $S_{11}$, $S_{12}$, $S_{21}$, and $S_{22}$).

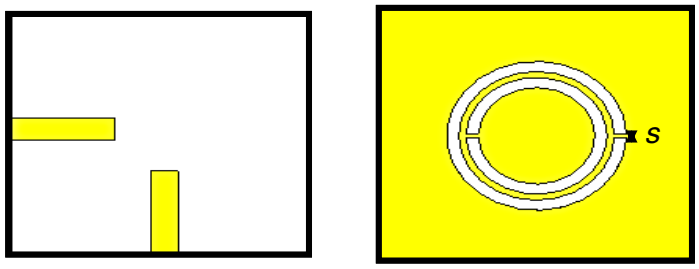


**Figure 5.** Antenna C.

In Figure 5, antenna C is depicted. Antenna C is designed by converting the dual rings into a CSRR, which is capable of creating an additional band of operation at 4.83 GHz. The return loss performance of antenna C is presented in Figure 6(a). In Figure 6(b), the effect of $S$ on the return loss of antenna C is presented. The $S$ value is increased in steps of 0.1 mm from 0.15 mm to 0.35 mm; from the figure, it is observed that the 5 GHz band is affected mainly compared to the lower band. This evidences that the etched CSRR is responsible for this band. $S = 0.25$ mm has suitable impedance matching with slightly higher bandwidth than the other two dimensions, and therefore, it is chosen for the final fabrication. In Figure 6(c), the effect of the CSRR ring width on the return loss parameter of antenna C is analyzed. The CSRR ring width ($ws$) is increased in steps of 0.25 mm from 0.75 mm to 1.25 mm.

From Figure 6(c) it is observed that as the ring width is increased, the resonant frequency gets decreased with a slight increase in bandwidth, due to the increase in additional capacitance. Figure 7 illustrates the plan of the massive MIMO antenna design for future 5G handsets. The design has been implemented on a $75 \times 150 \times 1.6\,\text{mm}^3$ — FR4 substrate. As illustrated, four elements of the dual-polarized radiators have been placed at the corner of the PCB. Each pair of microstrip lines will excite orthogonal polarizations to enhance the MIMO performances of the design. Antenna A has a single band operation from 3.50 GHz to 3.86 GHz. Antenna B has dual-band resonance from 3.40 GHz to 3.63 GHz and 4.84 GHz to 5.00 GHz. Antenna C has dual-band resonance with good impedance matching from 3.43 GHz to 3.62 GHz and 4.78 GHz to 5.04 GHz.

Figure 8, depicts the $S$ parameter of the proposed massive MIMO antenna. The bandwidth of the proposed antenna covers the sub-6 GHz band and LTE band. The isolation of the antenna is also better than 15 dB. The radiation pattern displayed in the figure clearly depicts that the antenna has omnidirectional pattern which covers the upper and lower sides of the handset. The antenna element is smaller with dual feeds/polarizations, as observed in the radiation pattern.

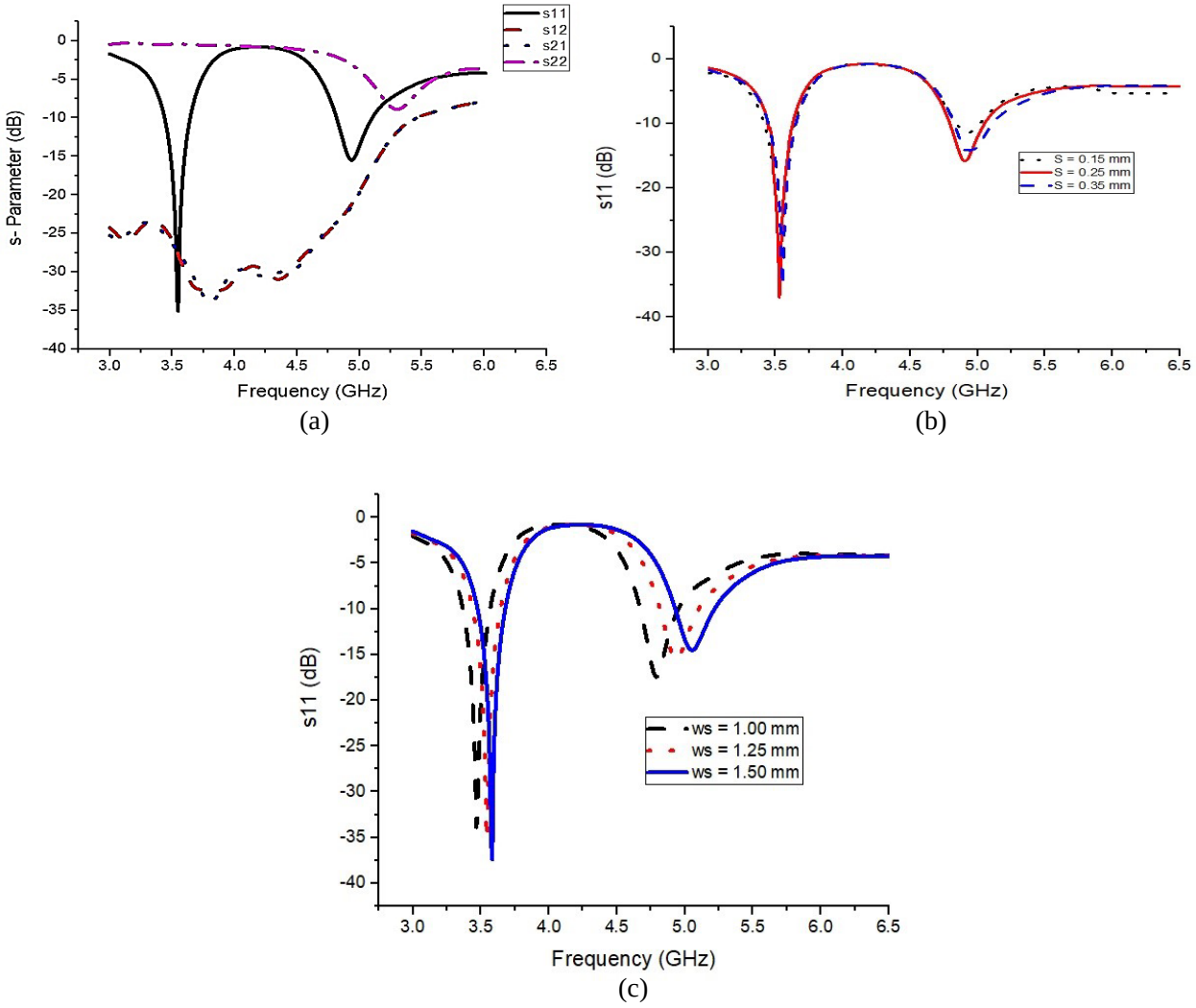


**Figure 6.** (a) Simulated $S$-parameter Antenna C (all $S_{11}$, $S_{12}$, $S_{21}$, and $S_{22}$). (b) Effect of $S$ on $S_{11}$ of antenna C. (c) Effect of $ws$ on $S_{11}$ of antenna C.

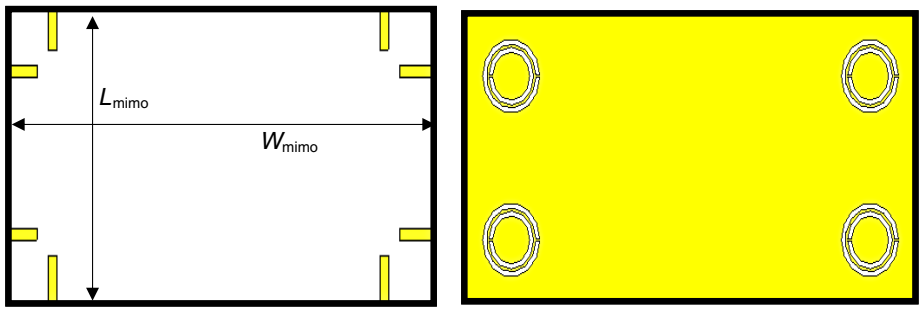


**Figure 7.** Proposed massive MIMO.

## 3. RESULT AND DISCUSSION

As illustrated, the CSRR resonators achieve good $S$-parameters with sufficient impedance bandwidth and low mutual coupling characteristics in the desired frequency range. The current distributions in the

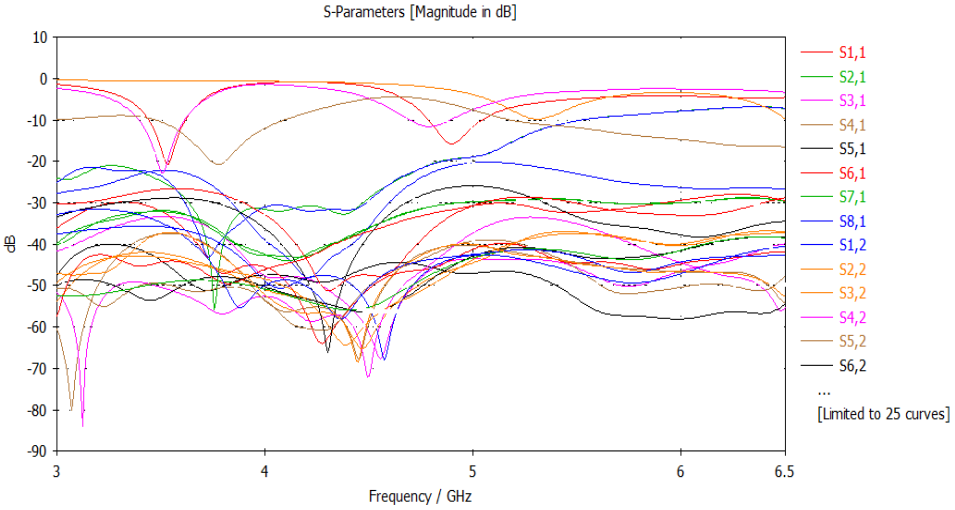


(a)

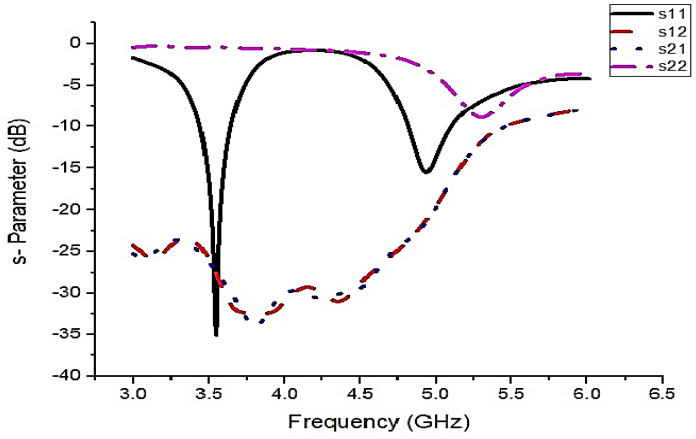


(b)

**Figure 8.** Reflection coefficient plot of the proposed antenna. (a) Simulated $8 \times 8$ MIMO (all $S$ parameters). (b) Simulated $8 \times 8$ MIMO (all $S_{11}$, $S_{12}$, $S_{21}$, and $S_{22}$).

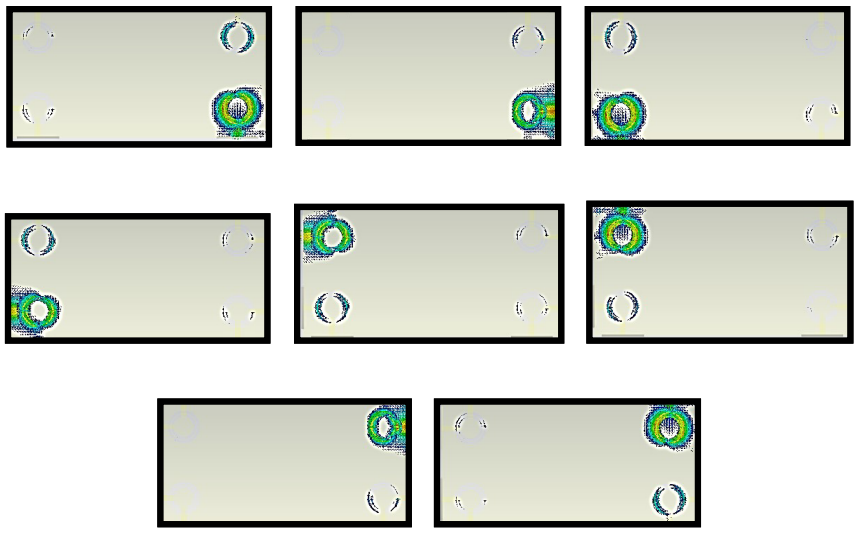

(a)

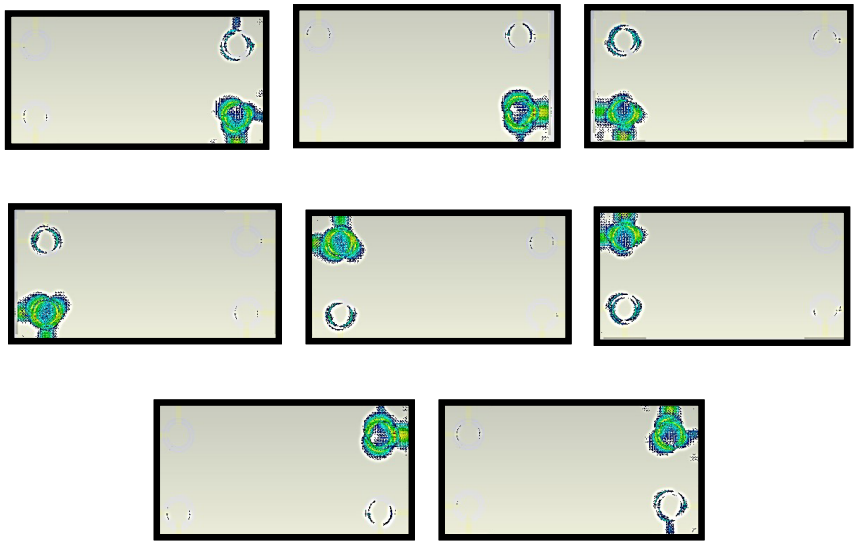

(b)

**Figure 9.** Surface current, (a) at 3.53 GHz, (b) at 4.89 GHz.

ground plane of the antenna at operating frequency (3.6 GHz) are illustrated in Figure 9. The currents are mainly distributed around the CSRR. As can be observed from Figure 9, for the different feeding ports of the antenna, the current flows are equal and opposite due to the polarization diversity function.

Figure 10 depicts the $E$ plane and $H$ plane radiation patterns at 3.53 GHz and 4.89 GHz. The proposed MIMO antenna can have an eight shaped dipole $E$ plane pattern and omnidirectional $H$ plane pattern. In Figure 11, the fabricated antenna in an anechoic chamber for the measurement of the radiation pattern is depicted. The VNA used for the $S$ parameter measurement is Anritsu S820E.

The simulated and measured results are presented in Figure 12. The deviation between the measured and simulated results is due to the fabrication and SMA connector error. In the above Figure 13, the directivity is plotted with respect to frequency, and the maximum directivity is 6.2 dBi. The maximum gain of the proposed antenna is above 4.32 dBi, presented in Figure 14, which compares the simulated gain with the measured one. In Table 1, the proposed MIMO antenna is compared with the already available antennas in the literature.

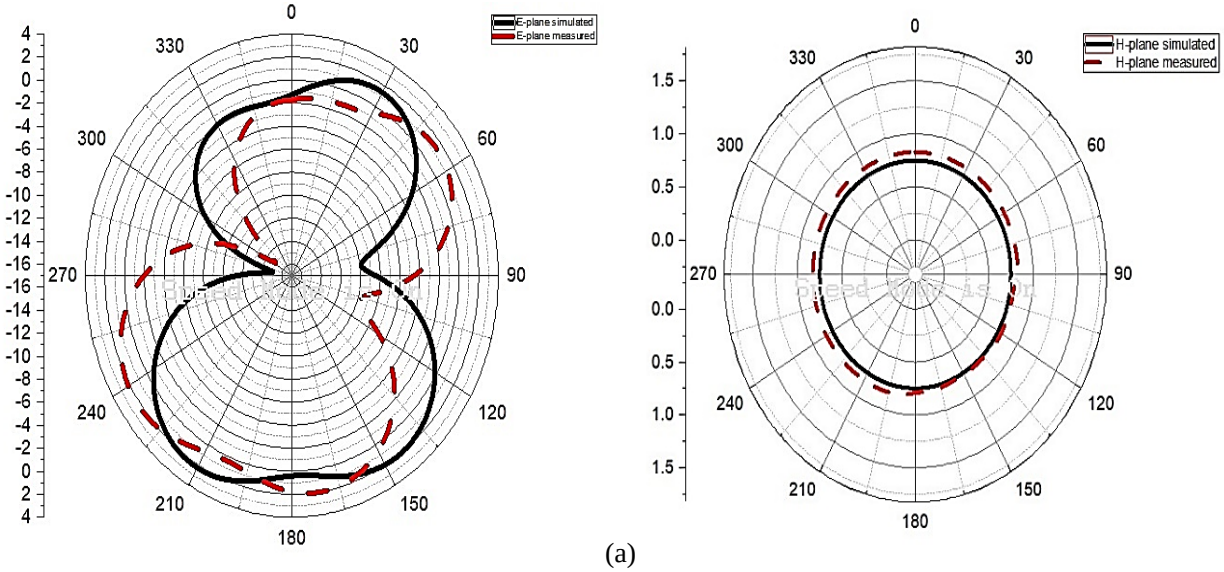


(a)

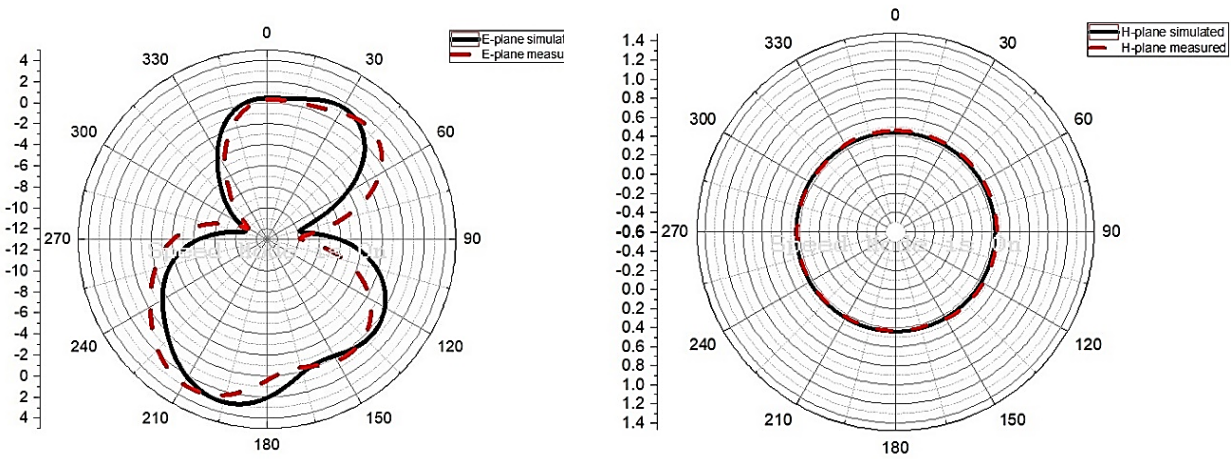


(b)

**Figure 10.** Radiation pattern $E$ plane and $H$ plane, (a) at 3.53 GHz, (b) at 4.89 GHz.

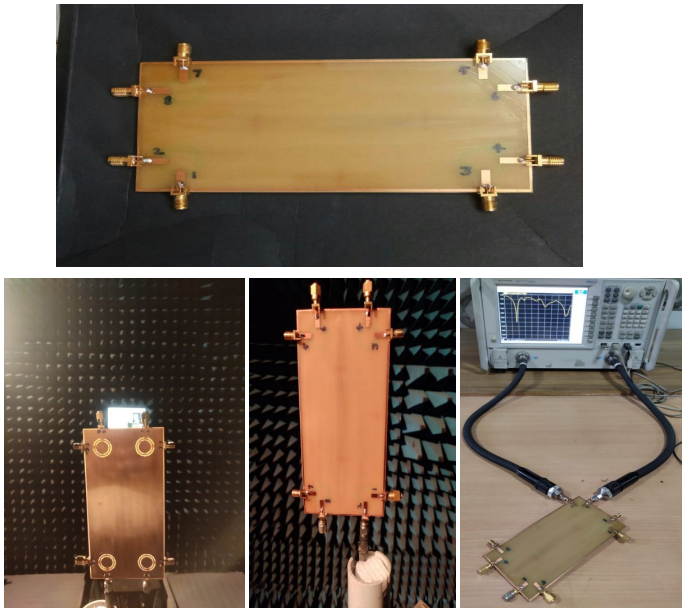

**Figure 11.** Antenna measurement setup and proposed MIMO in chamber.

The proposed structure exhibits a full coverage radiation pattern with polarization diversity, high radiation efficiency, good reasonable gain, and directivity. The proposed antenna is fabricated on a simple, cheap FR4 substrate. Another important parameter of MIMO antennas is envelope correlation coefficient (ECC). The diversity of a MIMO system can be evaluated using ECC, and its value should be less than 0.5. The ECC is given by

$$\rho_e(i,j,N) = \left| \frac{\sum_{n=1}^{N} S_{i,n}^{*} S_{n,j}}{\left| \prod_{k-i,j} \left( 1 - \sum_{n=1}^{N} S_{k,n}^{*} S_{n,j} \right) \right|} \right|$$

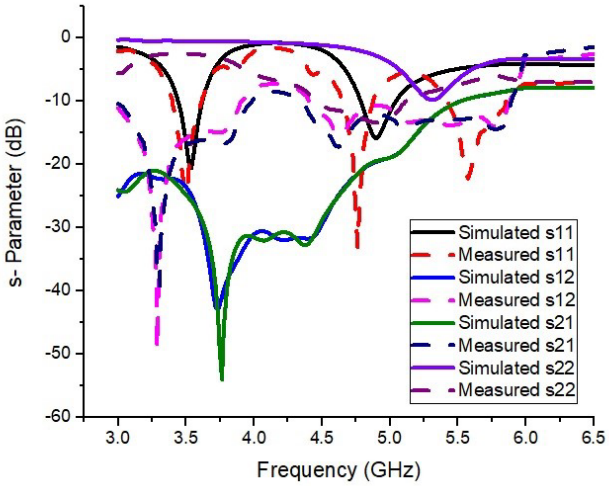


**Figure 12.** Measured vs simulated.

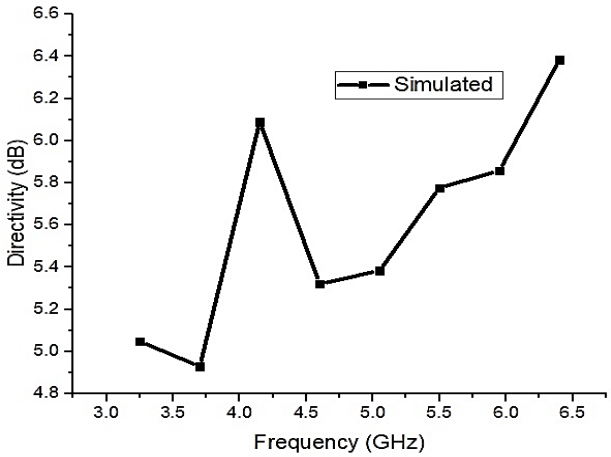


**Figure 13.** Directivity.

**Table 1.** Proposed antenna vs. antenna in the literature.

| Reference | Bandwidth | No. of Bands | Ground size | ECC | MIMO order | Isolation |
|---|---|---|---|---|---|---|
| [16] | 3.4 GHz to 3.6 GHz | 1 | 120 mm × 60 mm | NA | 8 | > 12 dB |
| [17] | 3.4 GHz to 3.6 GHz | 1 | 140 mm × 70 mm | < 0.1 | 10 | > 10 dB |
| [19] | 3.4 GHz to 3.6 GHz | 1 | 150 mm × 75 mm | < 0.3 | 16 | > 12 dB |
| [21] | 3.4 GHz to 3.6 GHz | 1 | 140 mm × 70 mm | < 0.2 | 8 | > 15 dB |
| [18] | 2.55 GHz to 2.65 GHz | 1 | 136 mm × 68 mm | < 0.15 | 8 | > 12 dB |
| [23] | 3.4 GHz to 3.6 GHz | 1 | 150 mm × 75 mm | < 0.15 | 8 | > 15 dB |
| Proposed | 3.43 GHz to 3.62 GHz & 4.78 GHz to 5.04 GHz | 2 | 150 mm × 75 mm | < 0.15 | 8 | > 15 dB |

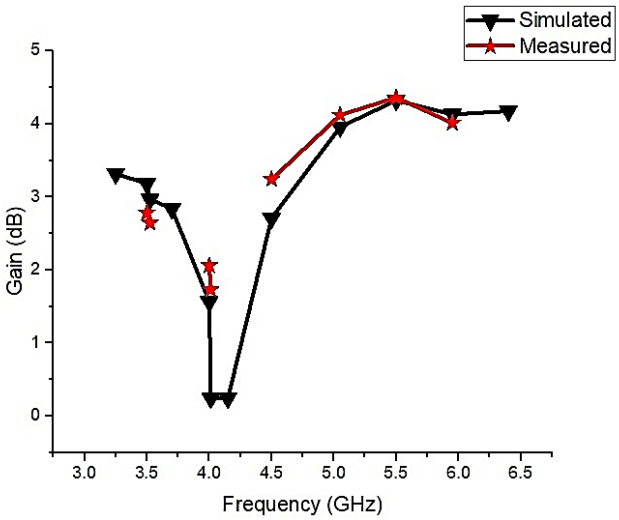


**Figure 14.** Simulated vs measured gain.

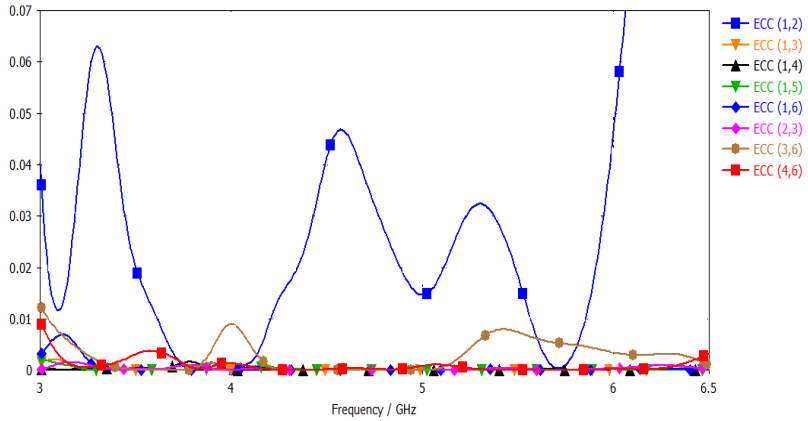


**Figure 15.** ECC of the proposed antenna.

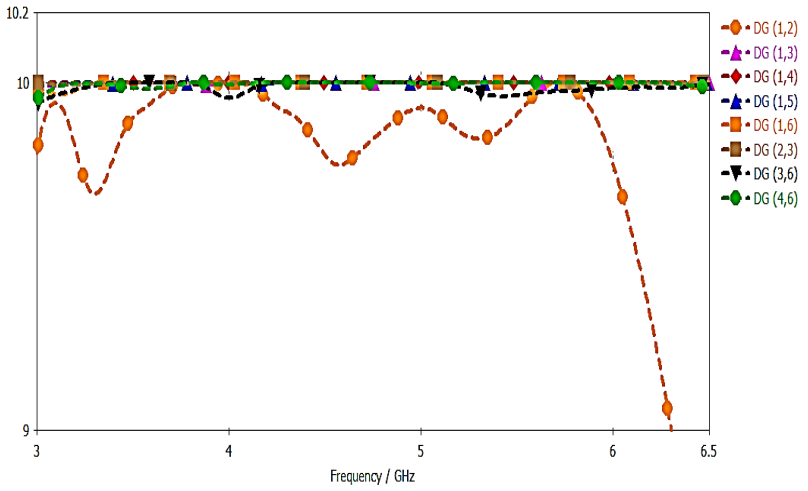


**Figure 16.** DG of the proposed antenna.

The simulated ECC of the proposed antenna is presented in Figure 15, and it is observed that the value of ECC is well below 0.07 in the entire operating frequency. In Figure 16, The simulated Diversity Gain (DG) is presented, and it is given by DG $= 10p$, where $p = (1 - |0.99e|^2)^{1/2}$. All the above reasons make the proposed antenna suitable for future 5G handsets.

## 4. CONCLUSION

In this article, a massive MIMO antenna for 5G smartphone applications is presented. The proposed structure has a Complementary SRR. The total dimension is 75 mm × 150 mm × 1.6 mm. 50-ohm dual microstrip feed lines placed orthogonal to each other are used to feed the CSRR. Due to this orthogonality, radiation diversity is easily achieved. The proposed structure is operated in dual bands from 3.43 GHz to 3.62 GHz and 4.78 GHz to 5.04 GHz. This simple structure gives good radiation diversity, reasonable gain, directivity, and a stable radiation pattern. Furthermore, good impedance bandwidth makes the proposed structure suitable for the sub-6 GHz 5G application, WLAN, LTE 42, 43, and LTE 46 U band applications.

## REFERENCES

1. Sharawi, M. S., *Printed MIMO Antenna Engineering*, Artech House, Norwood, MA, USA, 2014.
2. Parchin, N. O., et al., "8 × 8 MIMO antenna system with coupled-fed elements for 5G handsets," *The IET Conference on Antennas and Propagation (APC)*, Birmingham, UK, Nov. 11–12, 2019.
3. Ojaroudiparchin, N., et al., "Multi-layer 5G mobile phone antenna for multi-user MIMO communications," *TELFOR 2015*, Serbia, Nov. 2015.
4. Parchin, N. O., et al., "MM-wave phased array quasi-yagi antenna for the upcoming 5G cellular communications," *Applied Sciences*, Vol. 9, 1–14, 2019.
5. Gupta, P., "Evolvement of mobile generations: 1G to 5G," *International Journal for Technological Research in Engineering*, Vol. 1, 152–157, 2013.
6. Ojaroudi, N., "Design of microstrip antenna for 2.4/5.8 GHz RFID applications," *GeMic 2014*, RWTH Aachen University, Germany, 2014.
7. Zhang, S., K. Zhao, Z. Ying, and S. He, "Adaptive quad-element multi-wideband antenna array for user-effective LTE MIMO mobile terminals," *IEEE Trans. Antennas Propag.*, Vol. 61, No. 8, 4275–4283, Aug. 2013.
8. Andrews, J. G., et al., "What will 5G be?," *IEEE J. Sel. Area Comm.*, Vol. 32, No. 6, 1065–1082, Jun. 2014.
9. Li, H., Z. T. Miers, and B. K. Lau, "Design of orthogonal MIMO handset antennas based on characteristic mode manipulation at frequency bands below 1 GHz," *IEEE Trans. Antennas Propag.*, Vol. 62, No. 5, 2756–2766, May 2014.
10. Elshaer, H., M. N. Kulkarni, F. Boccardi, J. G. Andrews, and M. Dohler, "Downlink and uplink cell association with traditional macrocells and millimeter wave small cells," *IEEE Trans. Wirel. Commun.*, Vol. 15, No. 9, 6244–6258, Sep. 2016.
11. Holter, B., "On the capacity of the MIMO channel: A tutorial introduction," *Proc. IEEE Norwegian Symp. Signal Processing*, 167–172, 2001.
12. Zheng, L. and C. Tse, "Diversity and multiplexing: A fundamental trade-off in multiple antenna channels," *IEEE Trans. Inf. Theory*, Vol. 49, 1073–1096, May 2003.
13. WRC-15 Press Release, (Nov. 27, 2015). *World Radio Communication Conference Allocates Spectrum for Future Innovation.* [Online]. Available: http://www.itu.int/net/pressoffice/press_releases/2015/56.aspx.
14. Qualcomm. (Sep. 2015). *Making the Best Use of Licensed and Unlicensed Spectrum.* [Online]. Available: https://www.qualcomm.com/media/documents/files/making-the-best-useof-unlicensed-spectrum-presentation.pdf.
15. IMT-2020 (5G) Promotion Group. (Feb. 2015). *White Paper on 5G Concept.* [Online]. Available: http://www.imt-2020.org.cn/zh/documents/download.

16. Al-Hadi, A. A., J. Ilvonen, R. Valkonen, and V. Viikari, "Eight-element antenna array for diversity and MIMO mobile terminal in LTE 3500 MHz band," *Microw. Opt. Technol. Lett.*, Vol. 56, No. 6, 1323–1327, Jun. 2014.
17. Wong, K. L. and J. Y. Lu, "3.6-GHz 10-antenna array for MIMO operation in the smartphone," *Microw. Opt. Technol. Lett.*, Vol. 57, No. 7, 1699–1704, Jul. 2015.
18. Li, M. Y., et al., "Eight-port orthogonally dual-polarized antenna array for 5G smartphone applications," *IEEE Trans. Antennas Propag.*, Vol. 64, No. 9, 3820–3830, Sep. 2016.
19. Wong, K. L., J. Y. Lu, L. Y. Chen, W. Y. Li, and Y. L. Ban, "8-antenna and 16-antenna arrays using the quad-antenna linear array as a building block for the 3.5-GHz LTE MIMO operation in the smartphone," *Microw. Opt. Technol. Lett.*, Vol. 58, No. 1, 174–181, Jan. 2016.
20. Qin, Z., W. Geyi, M. Zhang, and J. Wang, "Printed eight-element MIMO system for compact and thin 5G mobile handest," *Electron. Lett.*, Vol. 52, No. 6, 416–418, Mar. 2016.
21. Ban, Y. L., C. Li, C. Y. D. Sim, G. Wu, and K. L. Wong, "4G/5G multiple antennas for future multi-mode smartphone applications," *IEEE Access*, Vol. 4, 2981–2988, Jul. 2016.
22. Wong, K. L., C. Y. Tsai, C. Y. Lu, D. M. Chian, and W. Y. Li, "Compact eight MIMO antennas for 5G smartphones and their MIMO capacity verification," *Proc. URSI Asia-Pac. Radio Sci. Conf.*, 1054–1056, Seoul, 2016.
23. Wong, K. L., C. Y. Tsai, and J. Y. Lu, "Two asymmetrically mirrored gap-coupled loop antennas as a compact building block for eight-antenna MIMO array in the future smartphone," *IEEE Trans. Antennas Propag.*, Vol. 65, No. 4, 1765–1778, Apr. 2017.
24. Prasad Jones Christydass, S., S. Praveen, S. Naveen Kumar, S. Rakesh Kumar, and M. Periakaruppan, "Design and implementation of tera-hertz antenna for high speed wireless communication," *Biosc. Biotech. Res. Comm. Special Issue*, Vol. 13, No. 3, May 2020.
25. Prasad Jones Christydass, S., B. Monisha, S. Shanthini, and R. Saranya, "Metamaterial inspired MIMO antenna for radar, satellite and terrestrial communications," *Biosc. Biotech. Res. Comm. Special Issue*, Vol. 13, No. 3, May 2020.
26. Prasad Jones Christydass, S. and N. Gunavathi, "Dual-band complementary split-ring resonator engraved rectangular monopole for GSM and WLAN/WiMAX /5G sub-6 GHz band (new radio band)," *Progress In Electromagnetics Research C*, Vol. 113, 251–263, 2021.
27. Shanthi, S., T. Jayasankar, S. Prasad Jones Christydass, and P. Maheswara Venkatesh, "Wearable textile antenna for GPS application," *International Journal of Scientific & Technology Research*, Vol. 8, No. 11, Nov. 2019.
28. Ramya, N., M. Sujatha, T. Jayasankar, and S. Prasad Jones Christydass, "Metamaterial inspired circular antenna with DGS for tetra band application," *International Journal of Control and Automation*, Vol. 13, No. 2, 877–882, Apr. 2020.
29. Prasad Jones Christydass, S. and N. Gunavathi, "Octa-band metamaterial inspired multiband monopole antenna for wireless application," *Progress In Electromagnetics Research C*, Vol. 113, 97–110, 2021.
30. Prasad Jones Christydass, S., A. S. Priyanka, S. Sugil, and R. Soundharya, "Metamaterial inspired bandpass filter for 5G application," *Biosc. Biotech. Res. Comm. Special Issue*, Vol. 13, No. 3, May 2020.
31. Prasad Jones Christydass, S. and N. Gunavathi, "A tri-band monopole antenna loaded with circular electric-inductive-capacitive metamaterial resonator for wireless application," *Applied Physics A*, Vol. 126, No. 10, 1–11, 2020.
32. Khan, M. S., D. E. Anagnostou, and R. M. Shubair, "A compact CSRR enabled UWB MIMO antenna," *IEEE Antennas and Wireless Propagation Letters*, Vol. 58, No. 6, 808–812, Aug. 2016.
33. Asif, S., J. Hansen, M. S. Khan, S. Walden, M. O. Jensen, and D. L. Ewert, "Design and in vivo test of a battery-less and fully wireless implantable asynchronous pacing system," *IEEE Transactions on Biomedical Engineering*, Vol. 63, No. 5, 1070–1081, Sep. 2015.

34. Iftikhar, A., R. M. Shubair, A.-D. Capobianco, and B. D. Braaten, "Eight-element compact UWB-MIMO/diversity antenna with WLAN band rejection for 3G/4G/5G communications," *IEEE Open Journal on Antennas and Propagation*, Vol. 1, 196–206, Apr. 2020.
35. Khan, M. U. and M. S. Sharawi, "A compact 8-element MIMO antenna system for 802.11ac WLAN applications," *2013 International Workshop on Antenna Technology (iWAT)*, 91–94, 2013, doi: 10.1109/IWAT.2013.6518306.
36. Prasad Jones Christydass, S. and N. Gunavathi, "Design of CSRR loaded multiband slotted rectangular patch antenna," *2017 IEEE Applied Electromagnetics Conference (AEMC)*, 1–2, 2017, doi: 10.1109/AEMC.2017.8325711.
37. Prasad Jones Christydass, S. and N. Gunavathi, "Co-directional CSRR inspired printed antenna for locomotive short range radar," *2017 International Conference on Inventive Computing and Informatics (ICICI)*, 627–630, 2017, doi: 10.1109/ICICI.2017.8365209.